Phytochemistry 169 (2020) 112161

Contents lists available at ScienceDirect

Phytochemistry

journal homepage: www.elsevier.com/locate/phytochem

Phytochemical and biological studies on rare and endangered plants endemic to China. Part XIV. **Structurally diverse terpenoids from the twigs and needles of the endangered plant *Picea brachytyla***

Wei Jiang[a], Juan Xiong[a], Yi Zang[b], Junmin Li[c], Ezzat E.A. Osman[a,d], Jing-Ya Li[b], Yu-Bo Zhou[b], Jia Li[b,**], Jin-Feng Hu[a,c,*]

[a] Department of Natural Products Chemistry, School of Pharmacy, Fudan University, Shanghai, 201203, PR China
[b] State Key Laboratory of Drug Research, Shanghai Institute of Materia Medica, Chinese Academy of Sciences, Shanghai, 201203, PR China
[c] Zhejiang Provincial Key Laboratory of Plant Evolutionary Ecology and Conservation, Taizhou University, Taizhou, 318000, Zhejiang, PR China
[d] Laboratory of Medicinal Chemistry, Theodor Bilharz Research Institute, Giza, 12411, Egypt

ARTICLE INFO

Keywords:
Picea brachytyla (Franch.) E.Pritz.
Pinaceae
Endangered plant
Terpenoids
Brachytylins
ATP citrate lyase (ACL)
SHP2 tyrosine phosphatase

ABSTRACT

A phytochemical investigation on the MeOH extract of the twigs and needles of the endangered plant *Picea brachytyla* led to the isolation and characterization of thirty-eight structurally diverse terpenoids. Seven of these molecules are previously undescribed, including three abietane-type (brachytylins A–C) and one labdane-type (brachytylin D) diterpenoids, an unseparated C-24 epimeric mixture of cycloartane-type triterpenoids (brachytylins E/F, ratio: 1:1), and a rare rearranged 12(1 → 6)-*abeo*-megastigmane glycoside (brachytylins G). Their structures and absolute configurations were determined by extensive spectroscopic (e.g., detailed 2D NMR and ECD) methods and/or X-ray diffraction analyses. All the isolates were evaluated for their inhibitory activities against the adenosine triphosphate (ATP)-citrate lyase (ACL) and the Src homology-2 domain containing protein tyrosine phosphatase-2 (SHP2). Among them, abiesadine J showed inhibitory effect against ACL, displaying an IC_{50} value of 17 μM. 3*S*,23*R*-Dihydroxycycloart-24-en-26-oic acid exhibited inhibitory effect on SHP2, with an IC_{50} value of 19 μM. Meanwhile, 3*R**,23*S**-dihydroxycycloart-24-en-26-oic acid was found to have inhibitory effects against both ACL and SHP2, with IC_{50} values of 16 and 12 μM, respectively.

1. Introduction

In general, plants from the Pinaceae family are trees (rarely shrubs), which can grow up to 2–100 m tall. Based on the morphology and the microscopical anatomy of the cones, pollen, seeds, wood, and leaves, this family is now divided into 11 genera (The Plant List, 2013): *Abies, Cathaya*, *Cedrus*, *Keteleeria*, *Larix*, *Picea, Pinus*, *Pseudolarix*, *Pseudotsuga*, *Tsuga*, and *Nothotsuga*. The last one was not listed in an earlier paper, in which the family was described to comprise 10 genera only (Hu et al., 2016a; Zheng and Fu, 1978). In fact, *Nothotsuga* contains only one species endemic to China, *N. longibracteata*. It is now regarded as a genus of coniferous trees in the family Pinaceae (The Plant List, 2013; Qiu et al., 2013). It is noteworthy to point out that Pinaceae is among the major plant families that produce high numbers of approved drugs (Zhu et al., 2011). However, the threats to the Pinaceae species have increased under anthropogenic activities and other massive ecological change impacts. There are 39 Pinaceae species recorded in the first volume of the China Plant Red Data Book (CPRDB) published in 1992 (Fu and Jin, 1992). The second volume of the CPRDB is currently under preparation and will contain more than six hundreds of additional endangered plants (López-Pujol et al., 2006), including increased numbers of Pinaceae species. Recently, several statistical surveys unveiled that the rare and endangered plants (REPs) could serve as better sources for drug discovery than other botanic sources (Zhu et al., 2011; Ibrahim et al., 2013). A pioneering phylogenetic study of the terrestrial plants showed that nature-derived drugs are mainly produced by specific drug-productive plant families, and most REPs species are in drug-producing families (Ibrahim et al., 2013). Therefore, there is a tremendous need to prioritize protection and utilization of these REPs species at extinction risk. Since 2013, a special program has been launched to systematically identify bioactive/novel natural products from REPs native to China (Xiong et al., 2018), and more attention has

* Corresponding author. Department of Natural Products Chemistry, School of Pharmacy, Fudan University, Shanghai, 201203, PR China.
** Corresponding author.
E-mail addresses: jli@simm.ac.cn (J. Li), jfhu@fudan.edu.cn (J.-F. Hu).

https://doi.org/10.1016/j.phytochem.2019.112161
Received 13 May 2019; Received in revised form 25 September 2019; Accepted 28 September 2019
0031-9422/ © 2019 Elsevier Ltd. All rights reserved.

Table 1
^{1}H NMR data (δ in ppm, J in Hz) for compounds **1–3** and **7**[a].

No.	**1**[b]	**2**[b]	**3**[c]	No.	**7**[d]
1	1.59 (m) (H-1_{ax})	1.63 (ddd, 12.6, 12.4, 4.2) (H-1_{ax})	1.63 (m) (H-1_{ax})	1	/
	2.38 (br d, 12.9) (H-1_{eq})	2.20 (br d, 12.4) (H-1_{eq})	2.18 (br d, 13.0) (H-1_{eq})	2	6.16 (s)
2	1.81 (br d, 13.6) (H-2_{eq})	1.77 (m) (H-2_{eq})	1.77 (m) (H-2_{eq})	3	/
	1.87 (qt-like, 13.6, 4.0) (H-2_{ax})	1.81 (m) (H-2_{ax})	1.81 (m) (H-2_{ax})	4	6.16 (s)
3	1.58 (m)	1.49 (m)	1.45 (m)	5	/
	1.43 (m)	1.43 (m)		6	/
5	2.31 (dd, 13.5, 4.4)	2.41 (dd, 2.9, 2.2)	2.40 (dd, 3.0, 2.7)	7	2.05 (m)
6	2.75 (dd, 18.1, 4.4) (H-6_{eq})	5.96 (dd, 9.7, 2.2)	5.93 (dd, 10.0, 2.7)		1.84 (m)
	2.69 (dd, 18.1, 13.5) (H-6_{ax})			8	1.02 (m)
7	/	6.56 (dd, 9.7, 2.9)	6.54 (dd, 10.0, 3.0)	9	3.81 (dd, 11.6, 5.5)
9	/	/	/	10	1.11 (d, 6.0)
11	7.52 (d, 8.3)	7.14 (d, 8.1)	7.10 (d, 8.0)	11	2.08 (s)
12	8.15 (dd, 8.3, 1.6)	7.24 (dd, 8.1, 1.9)	7.07 (dd, 8.0, 2.0)	12	1.32 (s)
14	8.54 (d, 1.6)	7.09 (d, 1.9)	6.93 (d, 2.0)	13	2.08 (s)
15	/	/	2.86 (sept, 7.0)	1′	4.28 (d, 7.8)
16	/	1.52 (s)	1.24 (d, 7.0)	2′	3.11 (dd, 8.0, 7.8)
17	2.64 (s)	1.53 (s)	1.24 (d, 7.0)	3′	3.35 (dd, 8.0, 7.0)
18a	3.48 (d, 11.0)	3.94 (d, 11.0)	3.94 (d, 11.0)	4′	3.26 (m)
18b	3.21 (d, 11.0)	3.88 (d, 11.0)	3.86 (d, 11.0)	5′	3.24 (m)
19	0.98 (s)	1.09 (s)	1.07 (s)	6′	3.87 (br d, 11.8)
20	1.30 (s)	1.09 (s)	1.08 (s)		3.67 (dd, 11.8, 5.1)
2′	/	2.63 (m)	2.63 (m)		
3′	/	2.63 (m)	2.63 (m)		
OMe	/	3.09 (s)	/		

[a] Assignments were made by a combination of 1D and 2D NMR experiments.
[b] Measured in $CDCl_3$ (600 MHz).
[c] Measured in $CDCl_3$ (400 MHz).
[d] Measured in CD_3OD (400 MHz).

been paid to the REPs species in the family Pinaceae (Hu et al., 2016a, 2017). A convictive example for the scientific community is that two rare sesquiterpenoids featuring a 6/6/5 ring system with an oxaspirolactone motif, beshanzuenones C and D, were obtained from the critically endangered Pinaceae plant *Abies beshanzuensis* (Hu et al., 2016b). The unique structures, the precious source, and the inhibiting activities of beshanzuenones against the protein tyrosine phosphatase 1B (PTP1B) have soon attracted the attention of scientists for their total syntheses and also provided valuable clues for producing new synthetic analogues with extended biological activity on the Src homology-2 domain containing protein tyrosine phosphatase-2 (SHP2) (Davis et al., 2018).

Among the 39 Pinaceae species in the first volume of the CPRDB (Fu and Jin, 1992), six belong to the genus *Picea* (*P. aurantiaca*, *P. brachytyla*, *P. montigena*, *P. neoveitchii*, *P. obovate*, and *P. smithiana*). As an endemic species to Qinling Mountains, *Picea. brachytyla* (Franch.) E.Pritz. has been protected as a 'vulnerable' plant in the CPRDB (Fu and Jin, 1992). The mountains geographically provide a special natural boundary between North and South China, and support a huge variety of plant species, some of which could be found nowhere else on Earth. *P. brachytyla* has never been phytochemically or pharmacologically investigated. In the course of our continuous interest in identifying bioactive compounds from REPs endemic to China (Xiong et al., 2018), the chemical constituents of the twigs and needles of this plant have been studied. As a result, a total of 38 structurally diverse terpenoids were isolated and characterized, including seven previously undescribed ones (**1–7**). Reported herein are their isolation, structure determination, and biological evaluations.

2. Results and discussion

The water-suspended 90% MeOH extract of the twigs and needles of *P. brachytyla* (10 kg) was fractionated successively with petroleum ether, EtOAc, and *n*-BuOH. Further chromatographic separation of the EtOAc and *n*-BuOH fractions afforded seven previously undescribed (**1–7**) and 31 known (**8–38**) terpenoids. By comparing the observed and reported spectroscopic data and physicochemical properties, the known structures were identified to be metaglyptin B (**8**) (Tu et al., 2019), 7-oxo-dehydroabietinol (**9**) (Tanaka et al., 1997), 7α,18-dihydroxy-dehydroabietanol (**10**) (Ohmoto et al., 1987), 7β,18-dihydroxy-dehydroabietanol (**11**) (Ohmoto et al., 1987), 18-succinoyloxyabieta-8,11,13-triene (**12**) (Raldugin et al., 2005), abiesadine J (**13**) (Yang et al., 2010), abiesadine Q (**14**) (Yang et al., 2010), 12β-hydroxyabieta-7,13-abietadien-18-oic acid (**15**) (Bleif et al., 2011), 12α-methoxy-abieta-7,13-dien-18-oic acid (**16**) (Wu et al., 2010), abietic acid (**17**) (Karlberg et al., 1988), 7-oxo-dehydroabietic acid (**18**) (Ayer and Macaulay, 1987), abieta-8,11,13,15-tetraen-18-oic acid (**19**) (Tanaka et al., 1997), 7α-methoxy-dehydroabietic acid (**20**) (Wu et al., 2010), dehydroabietic acid (**21**) (van Beek et al., 2007), 15-hydroxy-dehydroabietic acid (**22**) (Cheung et al., 1993), 15-methoxy-dehydroabietic acid (**23**) (Wang et al., 2010), 13*S*-hydroxy-9-oxo-9,10-*seco*-abiet-8(14)-en-18,10α-olide (**24**) (Tanaka et al., 2004), karamatsuic acid (**25**) (Ohtsu et al., 1999), 8(14)-podocarpen-13-oxo-18-oic acid (**26**) (Cheung et al., 1993), isopimaric acid (**27**) (Ryu et al., 2010), *cis*-abienol (**28**) (Hieda et al., 1983), labd-13(*E*)-ene-8α,15-diol (**29**) (Forster et al., 1985), 8-hydroxy-14,15-dinor-11(*Z*)-labden-13-one (**30**) (Hlubucek et al., 1974), (+)-3β-hydroxymanool (**31**) (Munesada et al., 1992), 3*S*,23*R*-dihydroxycycloart-24-en-26-oic acid (**32**) (Anjaneyulu et al., 1999), 3*S**,23*S**-dihydroxycycloart-24-en-26-oic acid (**33**) (Anjaneyulu et al., 1999), 3*R**,23*S**-dihydroxycycloart-24-en-26-oic acid (= 23-hydroxyisomangiferolic acid A, **34**) (Nguyen et al., 2017), 3*R**,23*R**-dihydroxycycloart-24-en-26-oic acid (= 23-hydroxyisomangiferolic acid B, **35**) (Nguyen et al., 2017), 6*S*,9*S*-dihydroxy-megastigma-4-en-9-*O*-β-D-glucopyranoside (**36**) (Wang et al., 2009), dilatanone (**37**) (Park et al., 2018), and 4-[4-hydroxy-6-(hydroxymethyl)-2,6-dimethyl-1-cyclohex-1-en-1-yl]butan-2-one (**38**) (Miyase et al., 1987), respectively. Metaglyptin B (**8**) was just recently reported from *Metasequoia glyptostroboides* (Tu et al., 2019), but the absolute configuration remaining unknown. In this study, its absolute configuration was unequivocally determined as (4*R*,5*R*,10*S*) by comparison of its ECD data ($\Delta\varepsilon_{211}$ +0.50, $\Delta\varepsilon_{227}$ +0.47) with those analogues reported in literature (Machumi et al., 2010).

Table 2
^{13}C NMR data (δ in ppm, 150 MHz) for compounds **1**–**4** and **7**[a].

No.	**1**[b]	**2**[b]	**3**[b]	**4**[b]	No.	**7**[c]
1	37.3	35.5	34.9	38.2	1	169.2
2	18.1	18.2	18.3	27.2	2	128.9
3	34.7	34.9	35.5	78.7	3	188.7
4	37.8	36.1	37.5	38.8	4	128.9
5	42.1	45.6	45.6	55.0	5	169.1
6	35.8	128.6	128.5	19.9	6	48.5
7	198.4	128.5	128.5	43.8	7	33.6
8	130.9	132.5	132.6	74.2	8	33.2
9	160.6	146.4	145.4	61.8	9	74.8
10	38.3	37.5	36.1	38.7	10	19.8
11	124.4	121.6	121.7	23.1	11	19.9
12	132.9	125.2	125.7	133.4	12	25.7
13	135.2	143.4	146.3	131.2	13	19.9
14	128.0	124.1	124.7	133.3	1′	102.0
15	197.3	76.6	33.6	114.1	2′	75.2
16		28.0	24.0	19.9	3′	78.2
17	26.7	27.8	24.0	24.4	4′	71.8
18	70.8	72.5	72.4	28.2	5′	77.9
19	17.3	18.2	18.2	15.4	6′	62.9
20	23.7	20.7	20.8	15.5		
1′		172.3	172.2			
2′		28.6	28.3			
3′		29.0	29.0			
4′		175.5	174.1			
OMe		50.7				

[a] Assignments were made by a combination of 1D and 2D NMR experiments.
[b] In $CDCl_3$.
[c] In CD_3OD.

Compound **1** was isolated as colorless needles (from CH_2Cl_2/*n*-hexane), and the molecular formula was determined to be $C_{19}H_{24}O_3$ based on the protonated ion at *m/z* 301.1800 $[M + H]^+$ (calcd for $C_{19}H_{25}O_3$, 301.1798) in its positive mode HRESIMS. The IR spectrum of **1** showed absorption bands (ν_{max}) attributable to hydroxy (3446 cm^{-1}), conjugated carbonyl (1690, 1676 cm^{-1}), and aryl (1594 cm^{-1}) functional groups. The presence of the latter two was consistent with the maximum absorption (λ_{max}) at 233, 257 (sh), and 295 nm in its UV spectrum (Ayer and Macaulay, 1987). Its ^{1}H NMR spectrum displayed signals of three methyl singlets [δ_H 0.98 (s, H_3-19), 1.30 (s, H_3-20), 2.64 (s, H_3-17)], a hydroxymethylene [δ_H 3.21 and 3.48 (ABq, J = 11.0 Hz, H_2-18)], and a typical AMX system for three aromatic protons at δ_H 7.52 (d, J = 8.3 Hz, H-11), 8.15 (dd, J = 8.3, 1.6 Hz, H-12), and 8.54 (d, J = 1.6 Hz, H-14) (Table 1). Analysis of the ^{13}C and HSQC NMR spectra of **1** revealed the presence of 19 carbon signals comprising three methyls, five methylenes (one oxygenated at δc 70.8, C-18), four methines [three olefinic at δc 124.4 (C-11), 128.0 (C-14), 132.9 (C-12)], five quaternary carbons [three olefinic at δc 130.9 (C-8), 135.2 (C-13), 160.6 (C-9)], and two keto-carbonyl carbons (δ_C 198.4, 197.3) (Table 2). The above data showed general features similar to those of 7-oxo-dehydroabietinol (**9**) (Tanaka et al., 1997), a co-occurring known abietane-type diterpenoid featuring the aromatic C ring with an AMX spin system. The most notable difference was that the isopropyl group in **9** was replaced by an acetyl group [δ_H: 2.64 (s, H_3-17), δ_C: 197.3 (C-15), 26.7 (C-17)] in **1**. This, in conjunction with its molecular formula, suggested that compound **1** is a C-17 norabietene derivative. The 2D structure of **1** was then confirmed by ^{1}H–^{1}H COSY (see Supporting Information) and HMBC (Fig. 4) data. The large proton-proton coupling constant (13.5 Hz) between H-5 and H-6_{ax} (Table 1) was indicative of a *trans* diaxial relationship between these two protons. The observed NOE correlations of H_3-19 with H_3-20 and H-6_{ax}, and of H_2-18 with H-5 and H-6_{eq} implied that H_3-20, H_3-19, and H-6_{ax} were cofacial, whereas H_2-18, H-5, and H-6_{eq} were all on the opposite side of the molecule. The ECD spectrum of **1** displayed a positive Cotton effect at 325 nm ($\Delta\varepsilon$ +1.26), which was in good accordance with those of reported (5*R*,10*S*)-7-oxo-abieta-8,11,13-trienes (Cambie et al., 1964; Snatzke, 1965), allowing the assignment of a 5*R*,10*S* configuration for **1**. The structure with the absolute configuration of **1** was finally established by a Ga-Kα X-ray crystallographic analysis (Fig. 5). Accordingly, compound **1**, named brachytylin A, was characterized as (4*R*,5*R*,10*S*)-7,15-dioxo-17-nor-abieta-8,11,13-trien-18-ol. Biogenetically, compound **1**, featuring an acetyl group at C-13, would be generated by an oxidative fission of the double bond between C-15 and C-17.

The molecular formula of brachytylin B (**2**) was established as $C_{25}H_{34}O_5$ based on ^{13}C NMR data and a *quasi*-molecular ion at *m/z* 413.2337 $[M - H]^-$ in its negative mode HRESIMS. Like compound **1**, signals assignable to the 1,2,4-trisubstitued aromatic C ring [δ_H 7.14 (d, J = 8.1 Hz, H-11), 7.24 (dd, J = 8.1, 1.9 Hz, H-12), and 7.09 (d, J = 1.9 Hz, H-14)] could be readily distinguished in its ^{1}H NMR spectrum (Table 1), implying an abieta-8,11,13-triene scaffold for **2**. The ^{1}H and ^{13}C NMR data of **2** were comparable to those of abiesadine J (**13**), a known dehydroabietanol congener with a succinoyloxy substituent at C-18 previously isolated from the conifer *Abies georgei* (Yang et al., 2010). Unlike **13**, a $\Delta^{6,7}$ double bond presented in the structure of **2**, which was evidenced from the olefinic protons resonated at δ_H 5.96 (dd, J = 9.7, 2.2 Hz, H-6) and 6.56 (dd, J = 9.7, 2.9 Hz, H-7), and the key HMBC correlations of H-6/C-8, H-7/C-5, and H-7/C-9 (Fig. 4). The relative configuration of **2** was determined (as depicted in Fig. 6) based on the key NOE correlations of H-2_{ax} with H_3-19 and H_3-20, and of H-5 with H_2-18. The absolute configuration of **2** was established by analysis of its ECD data. The Cotton effects ($\Delta\varepsilon_{217}$ –5.1, $\Delta\varepsilon_{258}$ +1.3) shown in its ECD spectrum (Fig. 7) were opposite to those of chlorabietin L (Xiong et al., 2016), an *ent*-abieta-6,8,11,13-tetraene diterpenoid from *Chloranthus oldhamii*. This suggested **2** is a normal abietane diterpenoid, in which C-10 has an *S* configuration and Me-20 is β-oriented (as depicted in Fig. 1). Thus, the structure of **2** was defined as (4*R*,5*R*,10*S*)-15-methoxy-18-succinoyloxy-abieta-6,8,11,13-tetraene.

With a deprotonated ion at *m/z* 383.2227 $[M - H]^-$ in its HRESIMS, brachytylin C (**3**) was found to have the molecular formula of $C_{24}H_{32}O_4$, with the loss of a methoxy group when compared with that of **2**. Consistent with this, the ^{1}H and ^{13}C NMR spectroscopic data of **3** were superimposable on those of **2**, except for the absence of the signals assigned to the methoxy group at C-15. The planar structure of **3** was further verified by the key HMBC correlations as shown in Fig. 4. Its relative configuration was also congruent with that of **2** based on the NOE correlations of H_3-20/H-1_{eq}, H_3-20/H-2_{ax}, H-2_{ax}/H_3-19, H_2-18/H-5, and H-5/H-1_{ax} (see Supporting Information). Similar Cotton effects in the ECD spectra (Fig. 7) of **3** ($\Delta\varepsilon_{217}$ –3.6, $\Delta\varepsilon_{258}$ +1.3) and **2** ($\Delta\varepsilon_{217}$ –5.1, $\Delta\varepsilon_{258}$ +1.3) suggested that they have the same absolute configurations (5*R*,10*S*) at C-5 and C-10. Compound **3** was thus identified as (4*R*,5*R*,10*S*)-18-succinoyloxy-abieta- 6,8,11,13-tetraene.

The positive mode HREIMS of brachytylin D (**4**) gave a sodium-adduct ion at *m/z* 329.2454 $[M + Na]^+$, indicating a molecular formula of $C_{20}H_{34}O_2$ with four degrees of unsaturation. In accordance with the molecular formula, the ^{13}C NMR spectrum of **4** displayed 20 carbon signals (Table 2) comprising five methyls, six methylenes [one olefinic at 114.1 (C-15)], five methines [one oxygenated at δ_C 78.7 (C-3), two olefinic at δ_C 133.4 (C-12) and 133.3 (C-14)], one oxygen-bearing tertiary carbon at δ_C 74.2 (C-8), and three quaternary carbons [one olefinic at δ_C 131.2 (C-13)]. Its ^{1}H NMR spectrum indicated the existence of four olefinic protons, among which three [δ_H 6.88 (dd, J = 17.2, 10.8 Hz, H-13), 5.23 (d, J = 17.2 Hz, H-14a), 5.13 (d, J = 10.8 Hz, H-14b)] were characteristic for a terminal double bond. Meanwhile, signals for an oxymethine proton resonated at δ_H 3.24 (dd, J = 11.5, 4.7 Hz, H-3) and five methyl singlets at δ_H 0.78 (s, H_3-19), 0.86 (s, H_3-20), 1.00 (s, H_3-18), 1.21 (s, H_3-17), and 1.81 (s, H_3-16) were observed (Table 1). The above data revealed that **4** is a bicyclic labdane-type diterpenoid similar to *cis*-abienol (**28**) (Hieda et al., 1983). A major difference between the two molecules was the appearance of an additional secondary hydroxy group in **4**, which was concluded to be at C-3 according to the key HMBC correlations from H_3-18 and H_3-19 to C-3 (Fig. 4). The H-3 was axial as it exhibited a large coupling constant

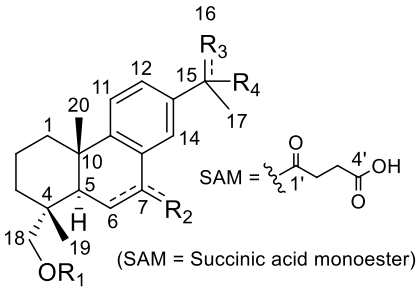

1: R_1 = H, R_2 = O, R_3, R_4 = O
2: R_1 = SAM, R_2 = H, R_3 = CH_3, R_4 = OCH_3, Δ^6
3: R_1 = SAM, R_2 = R_4 = H, R_3 = CH_3, Δ^6
8: R_1 = H, R_2 = H_2, R_3 = CH_3, R_4 = OCH_3
9: R_1 = R_4 = H, R_2 = O, R_3 = CH_3
10: R_1 = R_4 = H, R_2 = *ax*-OH, *eq*-H, R_3 = CH_3
11: R_1 = R_4 = H, R_2 = *eq*-OH, *ax*-H, R_3 = CH_3
12: R_1 = SAM, R_2 = H_2, R_3 = CH_3, R_4 = H
13: R_1 = SAM, R_2 = H_2, R_3 = CH_3, R_4 = OCH_3
14: R_1 = SAM, R_2 = O, R_3 = CH_3, R_4 = H

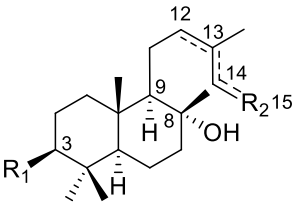

4: R_1 = OH, R_2 = CH_2, Δ^{12}, Δ^{14}
28: R_1 = H, R_2 = CH_2, Δ^{12}, Δ^{14}
29: R_1 = H, R_2 = CH_2OH, Δ^{13}

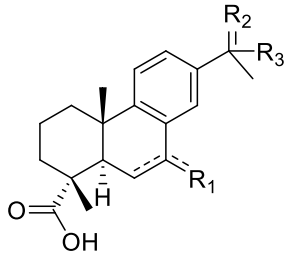

15: R = *eq*-OH
16: R = *ax*-OCH_3
17: R = H

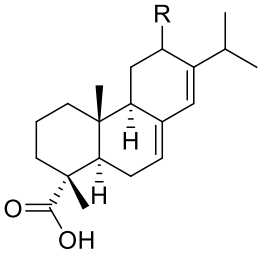

18: R_1 = O, R_2 = CH_3, R_3 = H
19: R_1 = H_2, R_2 = CH_2, Δ^{15}
20: R_1 = *ax*-OCH_3, *eq*-H, R_2 = CH_3, R_3 = H
21: R_1 = H_2, R_2 = CH_3, R_3 = H
22: R_1 = H_2, R_2 = CH_3, R_3 = OH
23: R_1 = H_2, R_2 = CH_3, R_3 = OCH_3

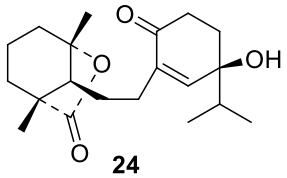

24

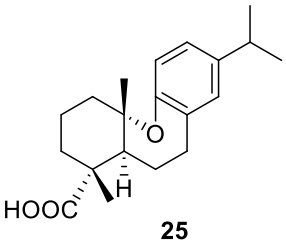

25

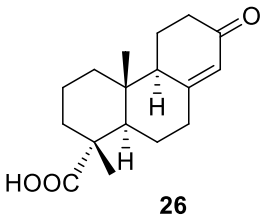

26

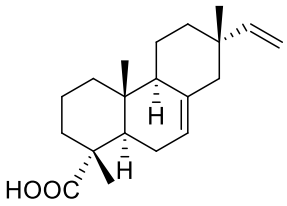

27

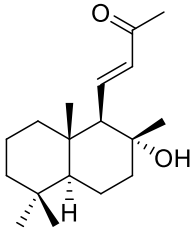

30

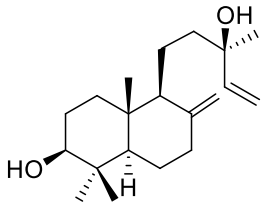

31

Fig. 1. Diterpenoids from *Picea brachytyla*.

(11.5 Hz) with the vicinal proton H-2_{ax}, implying an equatorial orientation for 3-OH. The relative configuration of the *trans*-decalin core of **4** was further confirmed by the clear NOE correlations of H-3/H-5, H-5/H-9, H-3/H_3-18, and H_3-19/H_3-20 (Fig. 6). An intense NOE cross-peak between H_3-20 and H_3-17 demonstrated the equatorial orientation of 8-OH. Like **28**, the clear NOE correlation between H-12 and H_3-16 (Fig. 6) was indicative of a 12*Z*-configuration for **4**. Therefore, compound **4** was ascertained as labda-12*Z*,14-dien-3,8-diol.

Compounds **5** and **6** were obtained as a pair of unseparated isomers (in a ratio of 1:1, Fig. 2), and both have the same molecular formula ($C_{30}H_{48}O_4$) based on their HRESIMS and ^{13}C NMR data (Table 3). Attempts to separate the mixture by employing different chromatographic methods especially HPLC, but failed (for details, see Experimental section). In the ^{1}H NMR spectrum of the mixture, signals at δ_H 0.34 and 0.55 (d, J = 4.0 Hz, H_2-19) were typical for a cyclopropane methylene group. Meanwhile, signals for five methyls [δ_H 0.81 (s, H_3-28), 0.88 (d, J = 6.0 Hz, H_3-21), 0.89 (s, H_3-30), and 0.97(s, H_3-18 and H_3-29)], two oxymethine protons [δ_H 3.30 (dd, J = 10.8, 4.8 Hz, H-3) and 4.38 (m, H-24)], and a pair of olefinic protons from a terminal methylene group [δ_H 6.37 (1H, br s) and 5.91/5.89 (each 0.5 H, br s)] were observed. These data suggested that both compounds **5** and **6** were cycloartane-type triterpenoids. Correspondingly, the ^{13}C NMR

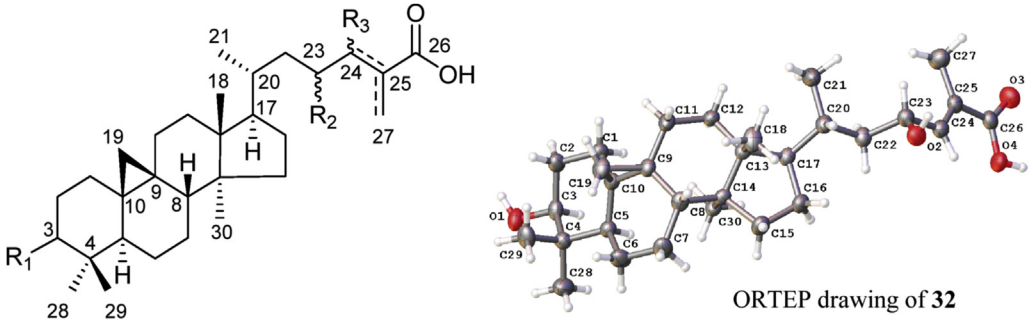

5/6: R_1 = *eq*-OH, R_2 = H, R_3 = OH, $\Delta^{25(27)}$, C-24: *R*/*S*
32: R_1 = *eq*-OH, R_2 = OH , Δ^{24}, C-23: *R*
33: R_1 = *eq*-OH, R_2 = OH , Δ^{24}, C-23: *S*
34: R_1 = *ax*-OH, R_2 = OH , Δ^{24}, C-23: *S*
35: R_1 = *ax*-OH, R_2 = OH , Δ^{24}, C-23: *R*

Fig. 2. Triterpenoids from *Picea brachytyla*.

data showed two sets of carbon resonances and each contained 30 signals (Table 1), including five methyls, twelve methylenes, six methines, six quaternary carbons, and one carboxyl carbon. Among them, the carbon resonances arising from the side chain (C-17 and C-21∼C-26, see Table 3) appeared in duplicate. The aforementioned NMR data for each component were comparable to those of 3*S*,23*R*-dihydroxycycloart-24*E*-en-26-oic acid (**32**) (Anjaneyulu et al., 1999), and variation was observed only in the nature of the side chain. The difference between **32** and **5/6** is that the Δ^{24} group in **32** was replaced by a terminal $\Delta^{25(27)}$ in **5/6**, which was evidenced from the 1D NMR data and HMBC correlations (Fig. 4). Meanwhile, the secondary hydroxy group at C-23 in **32** was shifted to C-24 in **5/6** as deduced from the HMBC correlations between this oxymethine carbon (δ_C 72.8/72.1, C-24) and H_2-27. A further comparison between the NMR data of compounds **5** and **6** (Table 3) revealed that they are C-24 epimeric isomers. Owing to the limited sample (1.4 mg in total), the absolute configuration at C-24 of **5** and **6** could not be defined. The relative configurations for the other chiral centers (i.e., C-3, C-5, C-8, C-9, C-10, C-13, C-14, and C-20) were determined to be the same as those of **32** by interpretation of the NOESY data (Fig. 5) and proton-proton coupling constants (Table 3). In particular, 3-OH was determined to be equatorially oriented from the large *J* value (10.8 Hz) between H-3 and H-2_{ax} and the NOE correlations of H-3 with H_3-28 and H-5. Thus, **5** and **6** were defined as a pair of C-24 epimers of 3*β*,24*ξ*-dihydroxycycloart-25-en-26-oic acid.

Along with compounds **5** and **6**, four related known cycloartane-type triterpenoids (**32–35**) were isolated and purified from the title plant. Compounds **32** and **33** were first reported from the Indian plant *Mangifera indica*, with the stereochemistry at C-23 being unknown (Anjaneyulu et al., 1999). In this study, the absolute configuration of **32**, especially for the stereochemistry at C-23 (23*R*), was undoubtedly established by the X-ray crystallography analysis (Fig. 2). Correspondingly, compound **33**, the 23-epimer of **32**, could be concluded to possess a (3*S*,23*S*) configuration. A direct comparison of the ^{1}H and ^{13}C NMR spectroscopic data of these two C-23 epimeric isomers (Table 3) revealed that appreciable differences could be found around C-23, especially for the coupling pattern of H-23 [appeared as br dd (*J* = 9.4, 8.0 Hz) for 23*R*-isomer, but ddd (*J* = 9.6, 9.3, 4.6 Hz) for the 23*S*-isomer]. Compounds **34** and **35**, another pair of C-23 epimers featuring a 3_{ax}-OH group, were previously isolated from *Trigona minor* (Nguyen et al., 2017), but their stereochemistry at C-23 are open until this study. As described above, the configuration of 23-OH was readily assigned as "23*S*" in **34**, whereas "23*R*" in **35** based on their 1D NMR data (Table 3).

The molecular formula $C_{19}H_{30}O_7$ of brachytylin G (**7**) was determined by its HRESIMS (*m/z* 371.2056 $[M + H]^+$, calcd for 371.2064) and ^{13}C NMR data (Table 2). The ^{1}H and ^{13}C NMR spectra showed characteristic signals for a *β*-glucose moiety, with the anomeric proton resonated at δ_H 4.28 (*J* = 7.8 Hz, H-1′) and six oxygen-bearing carbons at δ_C 102.0, 75.2, 78.2, 71.8, 77.9, and 62.9 (Tables 1 and 2). The remaining 13 carbon signals comprised four methyls (δ_C 19.8, 19.9, 19.9, and 25.7), two methylenes (δ_C 33.6 and 33.2), an oxymethine (δ_C 74.8), two olefinic methines (duplicate at δ_C 128.9), three quaternary carbons (δ_C 169.2, 169.1, and 48.5), and one carbonyl group (δ_C 188.7). These data were strongly reminiscent of the co-occurring megastigmane glycoside, 6*S*,9*S*-dihydroxymegastigma-4-ene-9-*O*-*β*-D-glucopyranoside (**36**) (Wang et al., 2009). Unlike the regular megastigmane skeleton (e.g., compounds **36–38**) with a geminal dimethyl group at C-1, Me-12 in the structure of **7** was shifted to the neighboring C-6 via a Wagner-Meerwein rearrangement (1,2-alkyl shift) (Hanson, 1991). This was

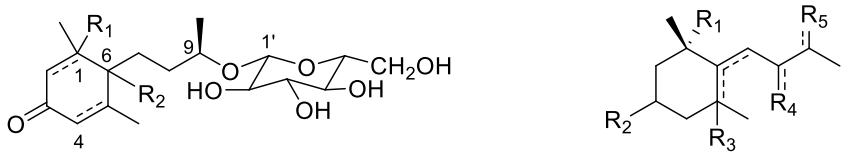

7: R_1 = NE, R_2 = CH_3, Δ^1, Δ^4
36: R_1 = CH_3, R_2 = OH, Δ^4, 6*S*
(NE = non-existent)

37: R_1 = CH_3, R_2 = R_3 = *eq*-OH, R_4 = R_5 = O, Δ^6
37a: R_1 = CH_3, R_2 = *eq*-OAc, R_3 = *eq*-OH, R_4 = R_5 = O, Δ^6
38: R_1 = CH_2OH, R_2 = *ax*-OH, R_4 = H_2, R_5 = O, Δ^5

Fig. 3. Megastigmene-type derivatives from *Picea brachytyla*.

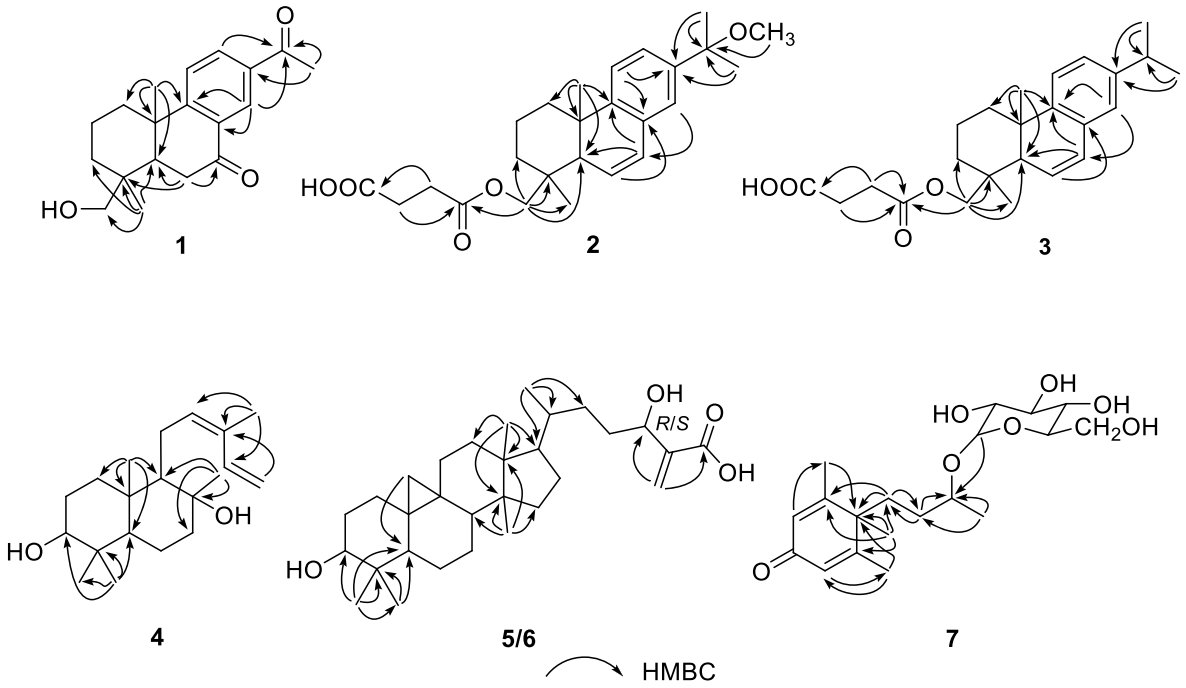

Fig. 4. Observed key HMBC correlations of **1**–**7**.

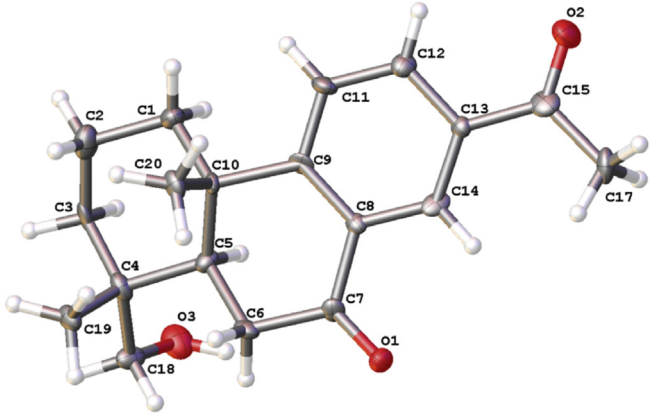

Fig. 5. ORTEP drawing of **1**.

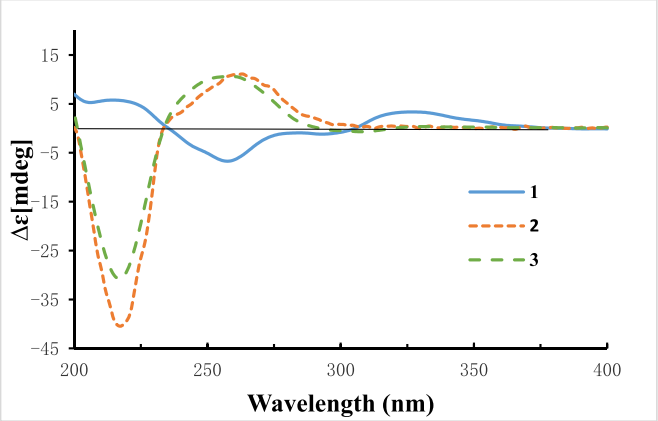

Fig. 7. Experimental ECD curves of **1**–**3** in MeOH.

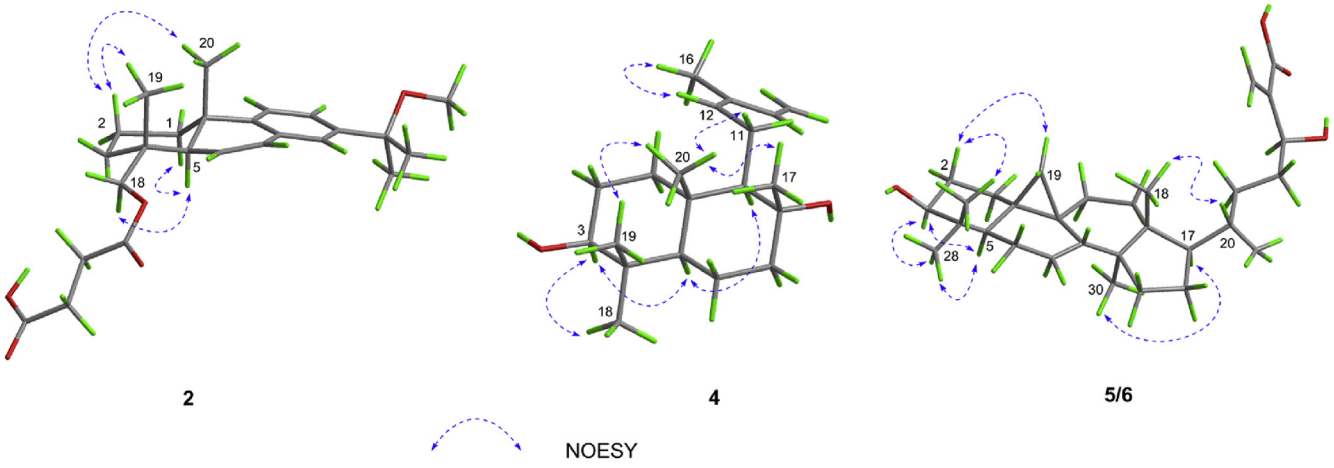

Fig. 6. Key NOE correlations of **2**, **4**, and **5**/**6**.

Table 3
^{1}H and ^{13}C NMR data (δ in ppm) for compounds **5/6** and **32–35**[a].

No.	**5/6**[b]		**32**[c]		**33**[c]		**34**[c]		**35**[c]	
	δ_H (J in Hz)[d]	δ_C [e]	δ_H (J in Hz)[d]	δ_C [e]	δ_H (J in Hz)[d]	δ_C [e]	δ_H (J in Hz)[d]	δ_C [e]	δ_H (J in Hz)[d]	δ_C [e]
1	1.81 (m)	32.9	2.05 (m)	33.3	2.02 (m)	33.2	1.88 (m)	28.7	1.86 (m)	28.7
	1.25 (m)		1.03 (m)		1.00 (m)		1.00 (m)		1.02 (m)	
2	1.76 (m)	30.4	1.69 (m)	31.0	1.68 (m)	31.0	1.95 (m)	29.6	1.93 (m)	29.6
	1.57 (m)		1.63 (m)		1.63 (m)		1.61 (m)		1.62 (m)	
3	3.30 (dd, 10.8, 4.8)	78.9	3.22 (dd, 10.6, 4.2)	79.5	3.21 (dd, 10.3, 3.8)	79.5	3.39 (br s)	77.7	3.39 (br s)	77.7
4	/	40.5	/	41.6	/	41.6	/	40.6	/	40.6
5	1.31 (m)	47.1	1.88 (m)	49.6	1.88 (m)	49.6	1.88 (m)	42.6	1.86 (m)	42.2
6	1.60 (m)	21.1	1.63 (m)	22.3	1.63 (m)	22.3	1.50 (m)	22.2	1.55 (m)	22.2
	0.80 (m)		0.84 (m)		0.84 (m)		0.80 (m)		0.81 (m)	
7	1.34 (m)	26.0	1.32 (m)	29.2	1.32 (m)	29.5	1.33 (m)	26.9	1.35 (m)	26.9
	1.10 (m)		1.11 (m)		1.12 (m)		1.15 (m)		1.13 (m)	
8	1.50 (m)	48.0	1.54 (m)	49.9	1.56 (m)	49.5	1.57 (m)	49.6	1.58 (m)	49.6
9	/	20.0	/	21.2	/	21.1	/	21.0	/	21.0
10	/	26.1	/	27.4	/	27.4	/	27.8	/	27.8
11	2.00 (m)	26.4	2.05 (m)	27.2	2.02 (m)	27.2	2.04 (m)	27.4	2.04 (m)	27.4
	1.11 (m)		1.17 (m)		1.19 (m)		1.16 (m)		1.17 (m)	
12	1.62 (m)	32.0	1.69 (m)	33.6	1.68 (m)	34.1	1.66 (m)	34.2	1.69 (m)	33.6
	1.49 (m)		1.36 (m)		1.41 (m)		1.66 (m)		1.69 (m)	
13	/	45.3	/	46.7	/	46.5	/	46.5	/	46.6
14	/	48.8	/	50.1	/	50.1	/	50.2	/	50.2
15	1.30 (m)	35.5	1.31 (m)	36.7	1.31 (m)	36.6	1.32 (m)	36.6	1.32 (m)	36.6
16	1.90 (m)	28.1	1.99 (m)	27.5	1.99 (m)	27.5	1.92 (m)	29.5	1.92 (m)	29.2
	1.31 (m)		1.73 (m)		1.87 (m)		1.31 (m)		1.31 (m)	
17	1.60 (m)	52.2/52.1	1.61 (m)	54.1	1.59 (m)	54.2	1.65 (m)	54.2	1.69 (m)	54.1
18	0.97 (s)	18.0	1.05 (s)	18.7	0.98 (s)	19.9	0.98 (s)	18.5	1.05 (s)	18.7
19	0.55 (d, 4.0)	29.9	0.58 (d, 3.8)	30.9	0.56 (d, 3.6)	30.8	0.52 (d, 3.5)	30.7	0.54 (d, 4.2)	30.7
	0.34 (d, 4.0)		0.37 (d, 3.8)		0.35 (d, 3.6)		0.37 (d, 3.5)		0.38 (d, 4.2)	
20	1.57 (m)	32.2/32.1	1.35 (m)	34.3	1.43 (m)	34.6	1.32 (m)	34.6	1.32 (m)	34.3
21	0.88 (d, 6.0)	18.3/18.2	0.99 (d, 6.0)	18.7	0.96 (d, 7.0)	19.8	0.97 (d, 6.0)	19.7	0.99 (d, 6.0)	18.6
22	1.44 (m)	35.9/35.7	1.68 (m)	44.1	1.68 (m)	44.9	1.66 (m)	44.9	1.66 (m)	44.1
	1.44 (m)		1.68 (m)		1.68 (m)		1.40 (m)		1.51 (m)	
23	1.75 (m)	33.0/32.9	4.54 (br dd, 9.4, 8.0)	66.7	4.53 (ddd, 9.6, 9.3, 4.6)	67.6	4.53 (ddd, 9.6, 9.4, 4.6)	67.6	4.54 (br dd, 9.2, 8.0)	66.7
24	4.38 (m)	72.8/72.1	6.69 (d, 8.0)	146.4	6.56 (d, 9.3)	145.0	6.56 (d, 9.4)	145.1	6.69 (d, 8.0)	146.4
25	/	141.5/141.2	/	127.7	/	129.6	/	129.6	/	127.7
26	/	168.2	/	171.5	/	171.5	/	171.5	/	171.5
27	6.37 (br s)	127.2/126.9	1.83 (s)	12.7	1.87 (s)	13.1	1.87 (s)	13.2	1.83 (s)	12.7
	5.91/5.89 (br s)									
28	0.81 (s)	14.0	0.81 (s)	14.7	0.80 (s)	14.7	0.92 (s)	26.6	0.92 (s)	26.6
29	0.97 (s)	25.4	0.95 (s)	26.1	0.94 (s)	26.4	0.88 (s)	21.9	0.89 (s)	21.9
30	0.89 (s)	19.3	0.94 (s)	19.8	0.94 (s)	18.5	0.96 (s)	19.9	0.95 (s)	19.8

[a] Assignments were made by a combination of 1D and 2D NMR experiments.
[b] In $CDCl_3$.
[c] In CD_3OD.
[d] Measured at 400 MHz.
[e] Measured at 600 MHz.

confirmed by the key HMBC correlations from H_3-12 to C-1, C-5, C-6, and C-7 (Fig. 4). In addition, the long conjugated system of $\Delta^{1,4}$-dien-3-one and the linkage position of the glucose were all verified by the HMBC correlations as depicted in Fig. 4. The stereochemistry of C-9 was characterized as *R** by comparing its chemical shift (δ_C 74.8) with those of related megastigmane glycosides reported in literature (9*R*: δ_C ~75.0; 9*S*: δ_C ~77.5) (Matsunami et al., 2010). The identification of the D-glucose moiety in the mass-limited **7** could be determined by analogy with the co-occurring **36** based on their similar NMR data and on a biogenetic consideration. In this study, acid hydrolysis of **36** gave a monosaccharide, which was identified to be D-glucose by direct comparison of its HPLC profile and optical rotation datum with those of an authentic sample (see Experimental section). Thus, the structure of **7** was elucidated as shown in Fig. 3. Such a rearranged 12(1 → 6)-*abeo*-megastigmane scaffold was rarely encountered in nature. Only balsamitone possessing such a backbone was previously obtained from the Turkish plant *Tanacetum balsamita* almost 45 years ago (Bohlmann et al., 1975).

Diabetes mellitus (DM) is a chronic metabolic disorder that occurs when there are raised levels of blood glucose ascribed to the body not producing any or enough hormone insulin and/or using insulin effectively (DeFronzo et al., 2015). Type 2 DM is the most common type of diabetes, accounting for approximately 90% of all DM cases (Yang et al., 2012). Recently, quite a few new enzyme-based targets related to type 2 DM have attracted great attentions (Chu et al., 2010; Dorenkamp et al., 2018; Li et al., 2019; Sun et al., 2019). Among them, the adenosine triphosphate (ATP)-citrate lyase (ACL) is a strategic enzymeαα linking both the glycolytic and lipidic metabolism (Granchi, 2018). The ACL serves as an epigenetic regulator to promote nephropathy in obesity and type 2 DM (Deb et al., 2017; Paton, 2017). Meanwhile, the Src homology-2 domain containing protein tyrosine phosphatase-2 (SHP2) is essential for receptor tyrosine kinase signaling and mitogen-activated protein kinase (MAPK) pathway activation. DM conditions exposure has been documented to be related with the upregulation of the expression of the SHP2 tyrosine phosphatase. Therefore, SHP2 is also regarded as a new target for improving monocyte function in Type 2 DM (Dorenkamp et al., 2018). Natural products have always played significant roles in the discovery of new chemical entities (NCEs) and drugs (Newman and Cragg, 2016). In this study, all the isolates were evaluated for their inhibitory activity against ACL using BMS 303141 as the positive control. Compounds **13**, **17**, **27**, and **34** showed moderate ACL inhibitory activities, with IC_{50} values ranging from 16 to 29 μM (Table 4). The

Table 4
Inhibitory activities of indicated compounds against ACL and SHP2.

Compound	IC_{50} (μM)[a]	
	ACL	SHP2
13	17 ± 2	> 50
17[b]	28 ± 5	> 50
27[b]	29 ± 3	> 50
32	> 50	19 ± 1
34	16 ± 2	12 ± 1
BMS 303141[c]	0.4 ± 0.1	N.T.[e]
Na_3VO_4[d]	N.T.[e]	0.9 ± 0.1

[a] The values (μM) indicate 50% ACL or SHP2 inhibitory effects. These data are expressed as the mean ± SEM of triplicate experiments.
[b] In this study, abietic acid (**17**) and isopimaric acid (**27**) showed comparable inhibitory effects against SHP2, when compared with literature data [**17** (IC_{50}): 0.32 ± 0.13; **27** (IC_{50}): 0.37 ± 0.13 mM (Hjortness et al., 2018)].
[c] Positive control for the ACL assay.
[d] Positive control for the SHP2 assay.
[e] N.T.: Not tested.

inhibitory effects against SHP2 were examined using DiFMUP as the substrate and Na_3VO_4 as the positive control. Compounds **32** and **34** exhibited inhibitory activities against SHP2, with IC_{50} values of 19 and 12 μM, respectively (Table 4). The rest of the isolates were found to be inactive (IC_{50} > 50 μM).

3. Concluding remarks

Terpenoids have been often encountered from the endangered plants in the family Pinaceae (Handa et al., 2013; Hu et al., 2016a, 2016b; 2017; Yang et al., 2010; Zhao et al., 2015). This is the first phytochemical investigation on the endangered coniferous plant *Picea brachytyla*, the Part XIV in our series of phytochemical and biological studies on REPs endemic to China (Xiong et al., 2018). From the MeOH extract of the twigs and needles of the title plant, a total of thirty-eight structurally diverse terpenoids were isolated and characterized, including seven previously undescribed ones. The absolute configurations of compounds **1** (abietane-type diterpenoid) and **32** (cycloartane-type triterpenoid) were finally confirmed based on the X-ray diffraction analyses, which could help to substantiate the absolute configurations of related compounds isolated in this study. Compound **7** features a rare 12(1 → 6)-*abeo*-megastigmane scaffold. Compounds **13**, **17**, **27**, and **34** showed moderate inhibitory effects on ACL, whereas compounds **32** and **34** exhibited significant inhibitory activities on SHP2. The above bioactive terpenoids may provide useful clues for discovery and development of new therapeutic or preventive agents for treatment of metabolic disorders (e.g., Type 2 DM) and other ACL or SHP2 related diseases. Moreover, the identification of new molecules from endangered plants reveals the importance in conservation efforts to prevent species diversity loss in the control of emerging targets.

4. Experimental

4.1. General experimental procedures

Optical rotations were measured on a Rudolf Autopol IV automatic polarimeter. UV spectra were recorded on a Hitachi U-2900E spectrophotometer. ECD spectra were recorded on a JASCO-810 CD spectrometer. IR measurements were performed on a Nicolet Is5 FT-IR spectrometer. X-ray data were collected on a Bruker D8 Venture diffractometer. NMR spectra were acquired on a Bruker Avance III 400 MHz or 600 MHz spectrometer, and the chemical shifts (δ) are given in ppm with reference to the solvent signals. HRESIMS data were recorded on an AB Sciex Triple TOF 5600 spectrometer. Semi-preparative HPLC was conducted on a Waters e2695 system equipped with a Sunfire C_{18} column (5 μm, 250 × 10 mm) and/or a TSK-Gel column (5 μm, 250 × 4.6 mm). Column chromatography (CC) was carried out using MCI gel CHP20P (75–150 μm, Mitsubishi Chemical Industries, Japan), silica gel (100–200 and 200–300 mesh, Ji-Yi-Da Silysia Chemical Ltd., Qingdao, PR China), and Sephadex LH-20 (GE Healthcare Bio-Sciences AB, Sweden). TLC analysis was conducted on precoated silica gel GF 254 plates (0.25 mm thick, Kang-Bi-Nuo Silysia Chemical Ltd., Yantai, PR China). Spots were visualized using UV light (254 nm) and by spraying with vanillin in sulfuric acid.

4.2. Plant material

The twigs and needles of *Picea brachytyla* (Franch.) E.Pritz. (Pinaceae) were collected from Taibai Mountains (33°88′ N, 107°41′ E), Shaanxi Province of PR China, in July 2017 (wet season). The plant was collected and identified by Mr. Gen-Lu Bai (Mei county botanist, Shaanxi Province). A voucher specimen (20170701) is deposited in the Department of Natural Product Chemistry, School of Pharmacy, Fudan University, PR China.

4.3. Extraction and isolation

The powdered twigs and needles of *P. brachytyla* (10 kg) were extracted four times with 90% MeOH (4 × 10 L) at room temperature. The MeOH extracts were combined and evaporated in vacuum to yield a brown residue (1 kg, semi-dry). The crude extract was suspended in H_2O (5 L) and partitioned successively with petroleum ether (PE), EtOAc, and *n*-BuOH. The entire EtOAc-soluble fraction (330 g) was subjected to column chromatography (CC) over silica gel [PE-EtOAc gradient (10:1–0:1, v/v) to EtOAc-MeOH gradient (20:1–0:1, v/v)], affording ten fractions (Fr.1 − Fr.10) based on TLC analysis. Fraction 4 (10.9 g) was separated over silica gel (PE-Acetone, from 30:1 to 1:1, v/v) to give eight subfractions, Fr.4.1–4.8. Subfraction Fr.4.3 (1.0 g) was preseparated by gel permeation chromatography on Sephadex LH-20 (in MeOH), followed by semi-preparative RP-HPLC [MeOH–H_2O (containing 0.05% TFA, v/v), 85:15], to afford compounds **15** (1.5 mg, t_R = 8.9 min), **19** (1.1 mg, t_R = 14.1 min), and **12** (4.4 mg, t_R = 38.7 min).

Fraction 5 (13.7 g) was fractionated on an MCI column with a stepwise gradient elution of MeOH–H_2O (50:50–100:0, v/v), and nine fractions (Fr. 5.1–5.9) were collected. Fr. 5.8 (1.2 g) was applied to a silica gel CC (stepwise PE-EtOAc, 20:1–1:1, v/v) to yield five fractions (Fr. 5.8.1–5.8.5). Fr.5.8.1 was separated via Sephadex LH-20 eluted in MeOH and semi-preparative HPLC [MeOH–H_2O (containing 0.05% TFA, v/v), 80:20] to yield compounds **22** (2.7 mg, t_R = 9.9 min), **23** (2.6 mg, t_R = 15.6 min), **18** (2.9 mg, t_R = 22.9 min), and **16** (1.5 mg, t_R = 28.5 min). Fr. 5.9 (1.9 g) was loaded onto silica gel CC eluted with PE-EtOAc (40:1–5:1, v/v) in a stepwise gradient of increasing polarity to afford five subfractions (Fr.5.9.1–5.9.5). Compound **27** (10.0 mg) was crystallized from fraction Fr.5.9.2 (300 mg), and the residue was further purified via a combination of silica gel CC (PE-CH_2Cl_2 1:1, v/v) and semi-preparative HPLC [MeOH–H_2O (containing 0.05% TFA, v/v), 92:8] to afford compounds **21** (2.0 mg, t_R = 14.8 min), **28** (7.8 mg, t_R = 18.9 min), and **17** (2.9 mg, t_R = 21.1 min).

Fraction 6 (23.7 g) was subjected to an MCI gel column eluted with gradients of MeOH–H_2O (30:70–100:0, v/v) to obtain eight fractions (Fr. 6.1–6.8). Subsequent separation of Fr. 6.4 (1.07 g) by CC over polyamide (MeOH–H_2O, 30:70–100:0, v/v) to give three subfractions (Fr. 6.4.1–6.4.3). After further purification by Sephadex LH-20 (in MeOH), subfraction Fr. 6.4.1 (0.87 g) gave four portions (Fr.6.4.1.1–6.4.1.4). Fr. 6.4.1.2 was chromatographed on silica gel CC and further purified by semi-preparative HPLC [MeOH–H_2O (containing 0.05% TFA, v/v), 75:25] to provide compounds **24** (4.1 mg, t_R = 10.6 min), **4** (2.0 mg, t_R = 20.7 min), **30** (5.0 mg, t_R = 36.5 min), and **31** (1.9 mg, t_R = 38.5 min). In a similar way, compounds **1** (4.0 mg, t_R = 10.2 min) and **26** (7.8 mg, t_R = 15.2 min) [HPLC mobile phase:

MeOH–H_2O (containing 0.05% TFA, v/v), 70:30] were obtained from Fr. 6.4.1.3 (100 mg). Fr. 6.5 was also processed in the same way as that described for Fr. 6.4, and the resultant Fr. 6.5.3 (260 mg) was subjected to semi-preparative HPLC (MeOH–H_2O, 80:20, v/v) to give compounds **11** (0.9 mg, t_R = 18.4 min), **29** (4.1 mg, t_R = 26.6 min), and **10** (2.6 mg, t_R = 29.7 min). Fr. 6.6 (910 mg) was repeatedly separated via Sephadex LH-20 (in MeOH) to afford five fractions (Fr. 6.6.1–6.6.5), and subfraction Fr. 6.6.3 (0.15 g) was further separated using silica gel CC eluted with PE-acetone (20:1–1:1, v/v) to obtain six fractions (Fr. 6.6.3.1 − Fr. 6.6.3.6), all of which were purified by semi-preparative HPLC. Consequently, compound **8** (2.2 mg, t_R = 10.6 min, MeOH–H_2O, 88:12, v/v) from Fr. 6.6.3.1, compounds **20** (1.5 mg, t_R = 17.5 min) and **13** (3.1 mg, t_R = 19.2 min) [MeOH–H_2O (containing 0.05% TFA), 80:20, v/v] from Fr. 6.6.3.2, compounds **32** (2.1 mg, t_R = 18.7 min), **33** (3.4 mg, t_R = 11.8 min), **34** (1.5 mg, t_R = 20.3 min), **35** (1.0 mg, t_R = 19.5 min), and **3** (1.0 mg, t_R = 24.2 min) [MeCN–H_2O (containing 0.05% TFA), 60:40, v/v] from Fr. 6.6.3.3, and compounds **14** (2.2 mg, t_R = 18.8 min) and the mixture of **5**/**6** (1.4 mg, t_R = 21.4 min) (MeOH–H_2O, 80:20, v/v) from Fr. 6.6.3.4, were obtained. The mixture of **5**/**6** showed a single spot on TLC in various developing solvent systems (e. g., PE: EtOAc 1:1, $CHCl_3$: MeOH 9:1, PE: acetone 2:1). Further chromatographic separations of this mixture on HPLC using different columns (e. g., Waters Sunfire C_{18}, Waters Xbrige, and Cosmosil cholester) with the mobile phase of either MeOH/H_2O or MeCN/H_2O were not achieved. Compounds **9** (2.0 mg, t_R = 20.1 min; MeCN–H_2O, 75:25, v/v) and **25** (1.4 mg, t_R = 23.5 min) [MeOH–H_2O (containing 0.05% TFA), 80:20, v/v] were isolated from Fr. 6.6.5. Fr. 6.7 (600 mg) was purified over Sephadex LH-20 gel CC and semi-preparative HPLC [MeOH–H_2O (containing 0.05% TFA, v/v), 86:14] to obtain compound **2** (2.3 mg, t_R = 14.2 min).

Fraction 8 (23.7 g) was subjected to a MCI gel column eluted with gradients of MeOH–H_2O (30:70–100:0, v/v) to obtain five fractions (Fr. 8.1–8.5). Fr. 8.2 (11.6 g) was further separated on silica gel CC eluted with CH_2Cl_2–MeOH (30:1–1:1, v/v) to obtain ten fractions (Fr. 8.2.1 − Fr. 8.2.10). Fr. 8.2.3 (910 mg) was purified using Sephadex LH-20 gel CC and then semi-preparative HPLC (MeOH–H_2O, 45:55, v/v) to obtain compounds **37** (3.4 mg, t_R = 10.9 min) and **38** (2.3 mg, t_R = 12.3 min).

The *n*-BuOH-soluble fraction was subjected to CC over silica gel eluted with CH_2Cl_2–MeOH (15:1–1:1) to afford eight fractions. The third fraction was resubmitted to Sephadex LH-20 and semipreparative HPLC (MeOH–H_2O, 30:70, v/v), yielding compounds **36** (7.2 mg, t_R = 17.8 min) and **7** (2.0 mg, t_R = 20.6 min).

4.3.1. Brachytylin A (1)

Colorless needles; $[\alpha]_D^{20}$ +2.2 (*c* 0.12, MeOH); UV (MeOH) λ_{max} (log ε) 233 (3.75), 257 (3.36, sh), 295 (2.70) nm; IR (KBr) ν_{max} 3446, 2965, 2923, 1690, 1676, 1594, 1412, 1384, 1212, 1182, 1075 cm^{-1}; ECD (*c* 2.0×10^{-3} M, MeOH) λ_{max} ($\Delta\varepsilon$) 215 (+2.19), 258 (−2.54), 325 (+1.26) nm; ^1H and ^{13}C NMR data, see Tables 1 and 2; HRESIMS $[M + H]^+$ *m/z* 301.1800 (calcd for $C_{19}H_{25}O_3$, 301.1798, Δ = +0.6 ppm).

4.3.2. Brachytylin B (2)

Yellow oil; $[\alpha]_D^{20}$ −20.0 (*c* 0.10, MeOH); UV (MeOH) λ_{max} (log ε) 219 (4.40), 265 (3.93) nm; IR (KBr) ν_{max} 3444, 2970, 2928, 2855, 1736, 1716, 1679, 1467, 1385, 1185 cm^{-1}; ECD (*c* 2.4×10^{-3} M, MeOH) λ_{max} ($\Delta\varepsilon$) 217 (−5.1), 258 (+1.3) nm; ^1H and ^{13}C NMR data, see Tables 1 and 2; HRESIMS $[M - H]^-$ *m/z* 413.2337 (calcd for $C_{25}H_{33}O_5$, 413.2333, Δ = +0.8 ppm).

4.3.3. Brachytylin C (3)

Yellow oil; $[\alpha]_D^{20}$ −4.0 (*c* 0.10, MeOH); UV (MeOH) λ_{max} (log ε) 218 (3.73), 265 (3.28) nm; IR (KBr) ν_{max} 3439, 2955, 2923, 2843, 1736, 1716, 1651, 1606, 1469, 1383, 1260, 1171 cm^{-1}; ECD (*c* 2.6×10^{-3} M, MeOH) λ_{max} ($\Delta\varepsilon$) 217 (−3.6), 258 (+1.3) nm; ^1H and ^{13}C NMR data, see Tables 1 and 2; HRESIMS $[M - H]^-$ *m/z* 383.2227 (calcd for $C_{24}H_{31}O_4$, 383.2228, Δ = −0.2 ppm).

4.3.4. Brachytylin D (4)

Colorless oil; $[\alpha]_D^{20}$ +4.1 (*c* 0.08, $CHCl_3$); UV (MeOH) λ_{max} (logε) 234 (3.73) nm; IR (KBr) ν_{max} 3450, 2950, 1640, 1460, 1445, 1115, 1085, 990, 940, 900 cm^{-1}; ^1H NMR (δ in ppm, *J* in Hz, in $CDCl_3$): 1.10 (ddd, *J* = 12.6, 12.4, 4.2 Hz, H-1_{ax}), 1.72 (m, H-1_{eq}), 1.87 (m, H-2a), 1.66 (m, H-2b), 3.24 (dd, *J* = 11.5, 4.7 Hz, H-3), 0.94 (dd, *J* = 12.0, 2.0 Hz, H-5), 1.67 (m, H-6a), 1.32 (m, H-6b), 1.87 (m, H-7a), 1.44 (m, H-7b), 1.30 (m, H-9), 2.44 (m, H-11a), 2.21 (m, H-11b), 5.48 (dd, *J* = 8.0, 8.0 Hz, H-12), 6.88 (dd, *J* = 17.2, 10.8 Hz, H-13), 5.23 (d, *J* = 17.2 Hz, H-14a), 5.13 (d, *J* = 10.8 Hz, H-14b), 1.81 (3H, s, H-16), 1.21 (3H, s, H-17), 1.00 (3H, s, H-18), 0.78 (3H, s, H-19), 0.86 (3H, s, H-20). For ^{13}C NMR data, see Table 2; HRESIMS $[M + Na]^+$ *m/z* 329.2454 (calcd for $C_{20}H_{34}O_2$, 329.2451, Δ = +0.8 ppm).

4.3.5. Brachytylins E and F (5 and 6)

Amorphous, white powder; $[\alpha]_D^{20}$ +12.8 (*c* 0.14, MeOH); UV (MeOH) λ_{max} (log ε) 204 (3.66) nm; IR (KBr) ν_{max} 3400, 3030, 2950, 2870, 1680, 1630, 1450 cm^{-1}; ^1H and ^{13}C NMR data, see Table 3; HRESIMS $[M - H]^-$ *m/z* 471.3483 (calcd for $C_{30}H_{47}O_4$, 471.3480, Δ = +0.7 ppm).

4.3.6. Brachytylin G (7)

Yellow gum; $[\alpha]_D^{20}$ −4.1 (*c* 0.09, MeOH); UV (MeOH) λ_{max} (log ε) 241 (3.99) nm; IR (KBr) ν_{max} 3446, 2924, 1656, 1619, 1380, 1075 cm^{-1}; ^1H and ^{13}C NMR data, see Tables 1 and 2; HRESIMS $[M + H]^+$ *m/z* 371.2056 (calcd for $C_{19}H_{31}O_7$, 371.2064, Δ = +2.3 ppm).

4.3.7. Metaglyptin B (8)

Amorphous, white powder; $[\alpha]_D^{20}$ +9.3 (*c* 0.14, $CHCl_3$); UV (MeCN) λ_{max} (log ε) 203 (3.73), 265 (2.22) nm; ECD (*c* 1.0×10^{-3} M, MeCN) λ_{max} ($\Delta\varepsilon$) 211 (+0.50), 221 (+0.47) nm; IR (KBr) ν_{max} 3447, 2975, 2927, 2853, 2361, 2337, 1738, 1682, 1463, 1383, 1255, 1164, 1070 cm^{-1}; ^1H and ^{13}C NMR data, see ref. (Tu et al., 2019); HRESIMS $[M+Na]^+$ *m/z* 339.2294 (calcd for $C_{21}H_{32}O_2Na$, 339.2295, Δ = +0.0 ppm).

4.3.8. 3S,23R-dihydroxycycloart-24-en-26-oic acid (32)

Amorphous, white powder; $[\alpha]_D^{20}$ +38.0 (*c* 0.10, MeOH); ^1H and ^{13}C NMR data, see Table 3; ESIMS $[M - H]^-$ *m/z* 470.8.

4.3.9. 3S*,23S*-dihydroxycycloart-24-en-26-oic acid (33)

Amorphous, white powder; $[\alpha]_D^{20}$ +48.0 (*c* 0.10, MeOH); ^1H and ^{13}C NMR data, see Table 3; ESIMS $[M - H]^-$ *m/z* 471.0.

4.3.10. 3R*,23S*-dihydroxycycloart-24-en-26-oic acid (34)

Amorphous, white powder; $[\alpha]_D^{20}$ +36.0 (*c* 0.15, MeOH); ^1H and ^{13}C NMR data, see Table 3; ESIMS $[M - H]^-$ *m/z* 470.8.

4.3.11. 3R*,23R*-dihydroxycycloart-24-en-26-oic acid (35)

Amorphous, white powder; $[\alpha]_D^{20}$ +12.9 (*c* 0.08, MeOH); ^1H and ^{13}C NMR data, see Table 3; ESIMS $[M - H]^-$ *m/z* 471.2.

4.3.12. X-ray crystallographic analysis of 1 and 32

X-ray crystallographic data for **1**: $C_{19}H_{24}O_3$, colorless crystals obtained from a solution of CH_2Cl_2/*n*-hexane (1:10, v/v), *M* = 300.38, Trigonal, Space group $P3_2$, *a* = 20.1158(2) Å, *b* = 20.1158(2) Å, *c* = 6.77244(9) Å, $\alpha = \beta = 90.00°$, $\gamma = 120.00°$, *V* = 2373.28(6) $Å^3$, *Z* = 6, D_{calcd} = 1.261 Mg/m^3, μ (Ga Kα) = 1.34139 Å, crystal size 0.12 × 0.05 × 0.03 mm^3, F (000) = 972, 33480 reflections collected, 5994 independent reflections (R_{int} = 0.0578), R_1 = 0.0891 [$I > 2\sigma(I)$], wR_2 = 0.2464 [$I > 2\sigma(I)$], R_1 = 0.0899 (all data), wR_2 = 0.2479 (all data), goodness of fit = 1.050, Flack parameter = 0.11(9).

X-ray crystallographic data for **32**: $C_{30}H_{48}O_4$, colorless crystals

obtained from MeOH, M = 472.68, monoclinic, space group P_1 2_1 1, a = 7.1450(2) Å, b = 11.3122(3) Å, c = 17.2791(5) Å, α = 90.00°, β = 100.64°, γ = 90.00°, V = 1372.59(7) Å^3, Z = 2, D_{calcd} = 1.144 Mg/m^3, μ (Ga Kα) = 1.34139 Å, crystal size 0.1 × 0.03 × 0.01 mm^3, F (000) = 520, 19,450 reflections collected, 5197 independent reflections (R_{int} = 0.0531), R_1 = 0.0391 [$I > 2\sigma(I)$], wR_2 = 0.0952 [$I > 2\sigma(I)$], R_1 = 0.0452 (all data), wR_2 = 0.1006 (all data), goodness of fit = 1.051, Flack parameter = −0.04(11).

The crystal structures of compounds **1** and **32** were solved by direct methods using SHELXT. Refinements were performed with SHELXL-2015 using full-matrix least-squares calculations on F^2, with anisotropic displacement parameters for all the non-hydrogen atoms. The hydrogen atom positions were geometrically idealized and allowed to ride on their parent atoms. CCDC-1912386 (**1**) and CCDC-1910919 (**32**), containing the supplementary crystallographic data, can be obtained free of charge from the Cambridge Crystallographic Data Centre via www.ccdc.cam.ac.uk/data_request/cif.

4.4. Acid hydrolysis of compound *36*

Compound **36** (3.0 mg) was hydrolyzed with 2 M aqueous CF_3COOH (TFA). After refluxing at 105 °C for 6 h, it was cooled to room temperature, and the solution was extracted with $CHCl_3$. The aqueous phase was concentrated to yield glucose (0.8 mg), which was identified by HPLC-ELSD using a TSK-Gel column (mobile phase: H_2O; flow rate: 1 mL/min; t_R = 10.1 min), with the authentic sample of D-glucose (Batch # 088K00391, Sigma-Aldrich) as a standard. The D-configuration was confirmed based on its optical rotation value of $[\alpha]_D^{20}$ +55.6 (c 0.08, H_2O) [ref. $[\alpha]_D^{20}$ +80.0 (c 0.1, H_2O)] (Hu et al., 2017).

4.5. Preparation of acetate *37a*

To a solution of **37** (1.5 mg) in 1 mL of dry pyridine was added six drops of $(CH_3CO)_2O$. This mixture was stirred at room temperature overnight and concentrated under reduced pressure to give a residue, which was purified by semi-preparative HPLC (MeOH–H_2O, 60:40, v/v) to furnish an acetate **37a** (1.9 mg). Compound **37a**, $[\alpha]_D^{20}$ −20.2 (c 0.10, MeOH); ECD (c 3.5 × 10^{-3} M, MeOH) λ_{max} ($\Delta\epsilon$) 228 (+3.3), 255 (−2.6) nm; ^{1}H NMR (400 MHz, in $CDCl_3$): 2.04 (br d, J = 13.0 Hz, H-2$_{eq}$), 1.48 (dd, overlapped, H-2$_{ax}$), 5.39 (m, H-3), 1.54 (dd, J = 13.0, 12.5 Hz, H-4$_{ax}$), 2.34 (br d, J = 13.0 Hz, H-4$_{eq}$), 5.88 (s, H-7), 2.20 (3H, s, H_3-10), 1.44 (3H, s, H_3-11), 1.17 (3H, s, H_3-12), 1.44 (3H, s, H_3-13), 2.06 (3H, s, -CO$\underline{CH_3}$); ^{13}C NMR (150 MHz, in $CDCl_3$): 36.0 (C-1), 45.0 (C-2), 67.4 (C-3), 45.0 (C-4), 72.0 (C-5), 118.4 (C-6), 100.9 (C-7), 209.5 (C-8), 198.0 (C-9), 26.4 (C-10), 28.9 (C-11), 31.6 (C-12), 30.8 (C-13), 170.4 (C-1′), 21.3 (C-2′).

4.6. ACL inhibitory activity assay

The assay was performed using ADP-Glo™ luminescence assay reagents. It measures ACL activity by quantification of the amount of ADP generated by the enzymatic reaction. The luminescent signal from the assay is correlated with the amount of ADP generated and is proportionally correlated with the amount of ACL activity (Koerner et al., 2017). The kinase assay was carried out in a 384-well plate (ProxiPlateTM-384 Plus, PerkinElmer) in a volume of 5 μL reaction mixture containing 2.0 μL of ACL, 2.0 μL of ATP, and 1.0 μL of test compounds with different concentrations. Reactions in each well were kept going for 30 min under 37 °C. After the enzymatic reaction, 2.5 μL of ADP-Glo™ reagent was added to each well to terminate the kinase reaction and deplete the unconsumed ATP within 60 min at room temperature. In the end, 5.0 μL of kinase detection reagent (reagent 2) was added to each well and incubated for 1 h to simultaneously convert ADP to ATP. The luminescence signal was measured using a PerkinElmer EnVision reader. The known inhibitor BMS 303141 (Koerner et al., 2017) was used as the positive control.

4.7. SHP2 inhibitory activity assay

Using the 8-difluoro-4-methylumbelliferyl phosphate (DiFMUP; Invitrogen, Carlsbad, CA) as the substrate, reaction buffer contained 60 mM Hepes (pH 7.0), 75 mM NaCl, 75 mM KCl, 0.05% Tween 20, 5 mM DTT, 1 mM EDTA, 25 μM DiFMUP, 0.1 μM GST-SHP2, and different concentrations of test compounds or DMSO in a total reaction volume of 50 μL in black 384-well plates. Reaction was initiated by addition of DiFMUP, and the incubation time was 30 min at 37 °C. DiFMUP fluorescence signal was measured at an excitation of 358 nm and an emission of 455 nm with a plate reader (PerkinElmer EnVision). Na_3VO_4 was used as the positive control (Dorenkamp et al., 2018; Wang et al., 2017).

Declaration of competing interest

The authors confirm that this article content has no conflict of interest.

Acknowledgements

This work was supported by NSFC grants (Nos. 21937002, 81773599, 21772025), a STCSM grant (No. 17430742200), and National Science and Technology Major Project for New Drug Research and Development of MOST (2019ZX09735002-005). WJ thanks Dr. Jerome M. Fox and his colleague Michael K. Hjortness (Department of Chemical and Biological Engineering, University of Colorado, USA) for sharing their valuable biological information of abietic acid and isopimaric acid against the protein tyrosine phosphatase SHP2. Their prompt replies via emails are highly appreciated.

Appendix A. Supplementary data

Supplementary data to this article can be found online at https://doi.org/10.1016/j.phytochem.2019.112161.

References

Anjaneyulu, V., Satyanarayana, P., Viswanadham, K.N., Jyothi, V.G., Nageswara Rao, K., Padhika, P., 1999. Triterpenoids from *Mangifera indica*. Phytochemistry 50, 1229–1236.
Ayer, W.A., Macaulay, J.B., 1987. Metabolites of the honey mushroom, *Armillaria mellea*. Can. J. Chem. 65, 7–14.
Bleif, S., Hannemann, F., Lisurek, M., von Kries, J.P., Zapp, J., Dietzen, M., Antes, I., Bernhardt, R., 2011. Identification of CYP106A2 as a regioselective allylic bacterial diterpene hydroxylase. Chembiochem 12, 576–582.
Bohlmann, F., Zdero, C., Schwarz, H., 1975. Naturally occurring terpene derivatives, XLVII. On a new sesquiterpene from *Tanaceturm balsumita* L.ssp. *balsamitoides* (Schultz Bip.) Grierson. Chem. Ber. 108, 1369–1372.
Cambie, R.C., Mander, L.N., Bose, A.K., Manhas, M.S., 1964. Rotatory dispersion and circular dichroism studies of some α-tetralones. Tetrahedron 20, 409–416.
Cheung, H.T.A., Miyase, T., Lenguyen, M.P., Smal, M.A., 1993. Further acidic constituents and neutral components of *Pinus massoniana* resin. Tetrahedron 49, 7903–7915.
Chu, K.Y., Lin, Y., Hendel, A., Kulpa, J.E., Brownsey, R.W., Johnson, J.D., 2010. ATP-citrate lyase reduction mediates palmitate-induced apoptosis in pancreatic beta cells. J. Biol. Chem. 285, 32606–32615.
Davis, D.C., Hoch, D.G., Wu, L., Abegg, D., Martin, B.S., Zhang, Z.-Y., Adibekian, A., Dai, M., 2018. Total synthesis, biological evaluation, and target identification of rare *Abies* sesquiterpenoids. J. Am. Chem. Soc. 140, 17465–17473.
Deb, D.K., Chen, Y., Sun, J., Wang, Y., Li, Y.C., 2017. ATP-citrate lyase is essential for high glucose-induced histone hyperacetylation and fibrogenic gene up-regulation in mesangial cells. Am. J. Physiol. Renal. Physiol. 313, 423–429.
DeFronzo, R.A., Ferrannini, E., Zimmet, P., Alberti, G., 2015. International Textbook of Diabetes Mellitus, fourth ed. Jonh Wiley & Sons, Ltd., Chichester.
Dorenkamp, M., Müller, J.P., Shanmuganathan, K.S., Schulten, H., Müller, N., Löffler, I., Müller, U.A., Wolf, G., Böhmer, F.-D., Godfrey, R., Waltenberger, J., 2018. Hyperglycaemia-induced methylglyoxal accumulation potentiates VEGF resistance of diabetic monocytes through the aberrant activation of tyrosine phosphatase SHP-2/SRC kinase signalling axis. Sci. Rep. 8, 14684.
Forster, P.G., Ghisalberti, E.L., Jefferies, P.R., 1985. Labdane diterpenes from an *Acacia* species. Phytochemistry 24, 2991–2993.
Fu, L.-G., Jin, J.-M., 1992. China Plant Red Data Book: Rare and Endangered Plants. Science Press, Beijing and New York.
Granchi, C., 2018. ATP citrate lyase (ACLY) inhibitors: an anti-cancer strategy at the

crossroads of glucose and lipid metabolism. Eur. J. Med. Chem. 157, 1276–1291.
Handa, M., Murata, T., Kobayashi, K., Selenge, E., Miyase, T., Batkhuu, J., Yoshizaki, F., 2013. Lipase inhibitory and LDL anti-oxidative triterpenes from *Abies sibirica*. Phytochemistry 86, 168–175.
Hanson, J.R., 1991. Wagner- Meerwein rearrangements. Comp. Org. Syn. 3, 705–719.
Hieda, T., Mikami, Y., Obi, Y., Kisaki, T., 1983. Microbial transformation of the labdanes, *cis*-abienol and sclareol. Agric. Biol. Chem. 47, 243–250.
Hjortness, M.K., Riccardi, L., Hongdusit, A., Ruppe, A., Zhao, M., Kim, E.Y., Zwart, P.H., Sankaran, B., Arthanari, H., Sousa, M.C., De Vivo, M., Fox, J.M., 2018. Abietane-type diterpenoids inhibit protein tyrosine phosphatases by stabilizing an inactive enzyme conformation. Biochemi 57, 5886–5896.
Hlubucek, J.R., Aasen, A.J., Almqvist, S.-O., Enzell, C.R., 1974. Synthesis of 14,15-bisnor-8-hydroxylabd-11*E*-en-13-one, a new tobacco constituent. Acta Chem. Scand. B 28, 131–132.
Hu, C.-L., Xiong, J., Gao, L.-X., Li, J., Zeng, H., Zou, Y., Hu, J.-F., 2016a. Diterpenoids from the shed trunk barks of the endangered plant *Pinus dabeshanensis* and their PTP1B inhibitory effects. RSC Adv. 6, 60467–60478.
Hu, C.-L., Xiong, J., Li, J.-Y., Gao, L.-X., Wang, W.-X., Cheng, K.-J., Yang, G.-X., Li, J., Hu, J.-F., 2016b. Rare sesquiterpenoids from the shed trunk barks of the critically endangered plant *Abies beshanzuensis* and their bioactivities. Eur. J. Org. Chem. 2016, 1832–1835.
Hu, C.-L., Xiong, J., Wang, P.-P., Ma, G.-L., Tang, Y., Yang, G.-X., Li, J., Hu, J.-F., 2017. Diterpenoids from the needles and twigs of the cultivated endangered pine *Pinus kwangtungensis* and their PTP1B inhibitory effects. Phytochem. Lett. 20, 239–245.
Ibrahim, M.A., Na, M., Oh, J., Schinazi, R.F., McBrayer, T.R., Whitaker, T., Doerksen, R.J., Newman, D.J., Zachos, L.G., Hamann, M.T., 2013. Significance of endangered and threatened plant natural products in the control of human disease. Proc. Natl. Acad. Sci. U.S.A. 110, 16832–16837.
Karlberg, A.-T., Bohlinder, K., Boman, A., Hacksell, U., Hermansson, J., Jacobsson, S., Nilsson, J.L.G., 1988. Identification of 15-hydroperoxyabietic acid as a contact allergen in Portuguese colophony. J. Pharm. Pharmacol. 40, 42–47.
Koerner, S.K., Hanai, J.-I., Bai, S., Jernigan, F.E., Oki, M., Komaba, C., Shuto, E., Sukhatme, V.P., Sun, L., 2017. Design and synthesis of emodin derivatives as novel inhibitors of ATP-citrate lyase. Eur. J. Med. Chem. 126, 920–928.
Li, S., Qin, C., Cui, S., Xu, H., Wu, F., Wang, J., Su, M., Fang, X., Li, D., Jiao, Q., Zhang, M., Xia, C., Zhu, L., Wang, R., Li, J., Jiang, H., Zhao, Z., Li, J.-Y., Li, H., 2019. Discovery of a natural-product-derived preclinical candidate for once-weekly treatment of type 2 diabetes. J. Med. Chem. 62, 2348–2361.
López-Pujol, J., Zhang, F.-M., Ge, S., 2006. Plant biodiversity in China: richly varied, endangered, and in need of conservation. Biodivers. Conserv. 15, 3983–4026.
Machumi, F., Samoylenko, V., Yenesew, A., Derese, S., Midiwo, J.O., Wiggers, F.T., Jacob, M.R., Tekwani, B.L., Khan, S.I., Walker, L.A., Muhammad, I., 2010. Antimicrobial and antiparasitic abietane diterpenoids from the roots of *Clerodendrum eriophyllum*. Nat. Prod. Commun. 5, 853–858.
Matsunami, K., Otsuka, H., Takeda, Y., 2010. Structural revisions of blumenol C glucoside and byzantionoside B. Chem. Pharm. Bull. 58, 438–441.
Miyase, T., Ueno, A., Takizawa, N., Kobayashi, H., Oguchi, H., 1987. Studies on the glycosides of *Epimedium grandiflorum* Morr. var. *thunbergianum* (Miq.) NAKAI. II. Chem. Pharm. Bull. 35, 3713–3719.
Munesada, K., Siddiqui, H.L., Suga, T., 1992. Biologically active labdane-type diterpene glycosides from the root-stalks of *Gleichenia japonica*. Phytochemistry 31, 1533–1536.
Newman, D.J., Cragg, G.M., 2016. Natural products as sources of new drugs from 1981 to 2014. J. Nat. Prod. 79, 629–661.
Nguyen, H.X., Nguyen, M.T.T., Nguyen, N.T., Awale, S., 2017. Chemical constituents of propolis from Vietnamese *Trigona minor* and their antiausterity activity against the PANC-1 human pancreatic cancer cell line. J. Nat. Prod. 80, 2345–2352.
Ohmoto, T., Kanatani, K., Yamaguchi, K., 1987. Constituent of pollen. XIII. Constituents of *Cedrus deodara* loud. (2). Chem. Pharm. Bull. 35, 229–234.
Ohtsu, H., Tanaka, R., Matsunaga, S., Tokuda, H., Nishino, H., 1999. Anti-tumor-promoting rearranged abietane diterpenes from the leaves of *Larix kaempferi*. Planta Med. 65, 664–666.
Park, K.-J., Subedi, L., Kim, S.-Y., Lee, K.-R., 2018. Anti-inflammatory terpenoid derivatives from the twigs of *Syringa oblata* var. *dilatata*. Phytochem. Lett. 27, 183–186.
Paton, D.M., 2017. Bempedoic acid. ATP-citrate lyase inhibitor, AMPK activator, treatment of hypercholesterolemia. Drug Future 42, 201–208.
Qiu, Y., Liu, Y., Kang, M., Yi, G., Huang, H., 2013. Spatial and temporal population genetic variation and structure of *Nothotsuga longibracteata* (Pinaceae), a relic conifer species endemic to subtropical China. Genet. Mol. Biol. 36, 598–607.
Raldugin, V.A., Grishko, V.V., Kukina, T.P., Druganov, A.G., Shakirov, M.M., 2005. 18-Succinyloxyabieta-8,11,13-triene as a new component from green shoots of the Siberian fir. Russ. Chem. Bull., Int. Ed. 54, 1747–1748.
Ryu, Y.B., Jeong, H.J., Kim, J.H., Kim, Y.M., Park, J.-Y., Kim, D., Naguyen, T.T.H., Park, S.-J., Chang, J.S., Park, K.H., Rho, M.-C., Lee, W.S., 2010. Biflavonoids from *Torreya nucifera* displaying SARS-CoV 3CL^{pro} inhibition. Bioorg. Med. Chem. 18, 7940–7947.
Snatzke, G., 1965. Circular dichroismus-X: modifizierung der octantenregel für α,β-ungesättigte ketone: cisoide enone, dienone und arylketone. Tetrahedron 21, 439–448.
Sun, L., Wang, P., Xu, L., Gao, L., Li, J., Piao, H., 2019. Discovery of 1,3-diphenyl-1*H*-pyrazole derivatives containing rhodanine-3-alkanoic acid groups as potential PTP1B inhibitors. Bioorg. Med. Chem. Lett 29, 1187–1193.
Tanaka, R., Ohtsu, H., Matsunaga, S., 1997. Abietane diterpene acids and other constituents from the leaves of *Larix kaempferi*. Phytochemistry 46, 1051–1057.
Tanaka, R., Wada, S., Kinouchi, Y., Tokuda, H., Matsunaga, S., 2004. A new *seco*-abietane-type diterpene from the stem bark of *Picea glehni*. Planta Med. 70, 877–880.
The Plant List, 2013. Version 1.1. A working list for all plant species. http://www.theplantlist.org/1.1/browse/G/Pinaceae/, Accessed date: 26 April 2019.
Tu, W.-C., Qi, Y.-Y., Ding, L.-F., Yang, H., Liu, J.-X., Peng, L.-Y., Song, L.-D., Gong, X., Wu, X.-D., Zhao, Q.-S., 2019. Diterpenoids and sesquiterpenoids from the stem bark of *Metasequoia glyptostroboides*. Phytochemistry 161, 86–96.
van Beek, T.A., Claassen, F.W., Dorado, J., Godejohann, M., Sierra-Alvarez, R., Wijnberg, J.B.P.A., 2007. Fungal biotransformation products of dehydroabietic acid. J. Nat. Prod. 70, 154–159.
Wang, B., Ju, J., He, X.-F., Yuan, T., Yue, J.-M., 2010. Three new terpenoids from *Pinus yunnanensis*. Helv. Chim. Acta 93, 490–496.
Wang, W., Li, X.-C., Ali, Z., Khan, I.A., 2009. Two new C_{13} nor-isoprenoids from the leaves of *Casearia sylvestris*. Chem. Pharm. Bull. 57, 636–638.
Wang, W.-L., Chen, X.-Y., Gao, Y., Gao, L.-X., Sheng, L., Zhu, J., Xu, L., Ding, Z.-Z., Zhang, C., Li, J.-Y., Li, J., Zhou, Y.-B., 2017. Benzo[*c*][1,2,5]thiadiazole derivatives: a new class of potent Src homology-2 domain containing protein tyrosine phosphatase-2 (SHP2) inhibitors. Bioorg. Med. Chem. Lett 27, 5154–5157.
Wu, L., Li, Y.-L., Li, S.-M., Yang, X.-W., Xia, J.-H., Zhou, L., Zhang, W.-D., 2010. Systematic phytochemical investigation of *Abies spectabilis*. Chem. Pharm. Bull. 58, 1646–1649.
Xiong, J., Hong, Z.-L., Xu, P., Zou, Y. Yu, S.-B., Yang, G.-X., Hu, J.-F., 2016. *ent*-Abietane diterpenoids with anti-neuroinflammatory activity from the rare Chloranthaceae plant *Chloranthus oldhamii*. Org. Biomol. Chem. 14, 4678–4689.
Xiong, J., Wang, L.-J., Qian, J., Wang, P.-P., Wang, X.-J., Ma, G.-L., Zeng, H., Li, J., Hu, J.-F., 2018. Structurally diverse sesquiterpenoids from the endangered ornamental plant *Michelia shiluensis*. J. Nat. Prod. 81, 2195–2204.
Yang, W., Zhao, W., Xiao, J., Li, R., Zhang, P., Kissimova-Skarbek, K., Schneider, E., Jia, W., Ji, L., Guo, X., Shan, Z., Liu, J., Tian, H., Chen, L., Zhou, Z., Ji, Q., Ge, J., Chen, G., Brown, J., 2012. Medical care and payment for diabetes in China: enormous threat and great opportunity. PLoS One 7, e39513.
Yang, X.-W., Feng, L., Li, S.-M., Liu, X.-H., Li, Y.-L., Wu, L., Shen, Y.-H., Tian, J.-M., Zhang, X., Liu, X.-R., Wang, N., Liu, Y., Zhang, W.-D., 2010. Isolation, structure, and bioactivities of abiesadines A-Y, 25 new diterpenes from *Abies georgei* Orr. Bioorg. Med. Chem. 18, 744–754.
Zhao, Q.-Q., Song, Q.-Y., Jiang, K., Li, G.-D., Wei, W.-J., Li, Y., Gao, K., 2015. Spirochensilides A and B, two new rearranged triterpenoids from *Abies chensiensis*. Org. Lett. 17, 2760–2763.
Zheng, W.-J., Fu, L.-G., 1978. Flora of China, vol. 7. Science Press, Beijing, pp. 32–211.
Zhu, F., Qin, C., Tao, L., Liu, X., Shi, Z., Ma, X., Jia, J., Tan, Y., Cui, C., Lin, J., Tan, C., Jiang, Y., Chen, Y., 2011. Clustered patterns of species origins of nature-derived drugs and clues for future bioprospecting. Proc. Natl. Acad. Sci. U.S.A. 108, 12943–12948.